Pitkäniemi, Sami; Routimo, Mikko; Kukkola, Jarno; Pirsto, Ville; Pouresmaeil, Edris

An Approach Utilizing Converters for Locating Faults in LV Distribution Grids

Published in:
Proceedings of the 23rd European Conference on Power Electronics and Applications, EPE'21 ECCE Europe

Published: 25/10/2021

Document Version
Peer-reviewed accepted author manuscript, also known as Final accepted manuscript or Post-print

Please cite the original version:
Pitkäniemi, S., Routimo, M., Kukkola, J., Pirsto, V., & Pouresmaeil, E. (2021). An Approach Utilizing Converters for Locating Faults in LV Distribution Grids. In Proceedings of the 23rd European Conference on Power Electronics and Applications, EPE'21 ECCE Europe IEEE. https://ieeexplore.ieee.org/document/9570488

An Approach Utilizing Converters for Locating Faults in LV Distribution Grids

Sami Pitkäniemi, Mikko Routimo, Jarno Kukkola, Ville Pirsto, and Edris Pouresmaeil
Aalto University
Department of Electrical Engineering and Automation
Espoo, Finland
Email: mikko.routimo@aalto.fi
URL: https://www.aalto.fi

Keywords

≪Artificial intelligence≫, ≪Distributed generation≫, ≪Faults≫, ≪Grid-connected converter≫ ≪Impedance measurement≫, ≪Machine learning≫, ≪Power transmission≫, ≪Smart grids≫

Abstract

This paper proposes an approach for locating faults in a distribution grid by utilizing data measured and gathered by distributed converters. The data, comprising grid voltages and impedances from multiple locations, is processed using multinomial logistic regression, a machine learning algorithm, to classify a fault location in the grid. The algorithm is first trained with simulation data, followed by evaluation of its predictive performance using a set of test data previously unseen by the algorithm. The fault location accuracy of the proposed approach is found resonable and encourages further studies of the unused potential in the converters.

1. Introduction

Modern society is dependent on constant and reliable availability of electricity. Additionally, the regulations regarding the allowed outage times are tightening. This provides a challenge for the network operators, since the power grid is a large system covering a wide area and faults can occur anywhere within the network. In order to minimize the effect of faults, they need to be located, isolated, and repaired quickly. Several different methods for locating faults in the grid have been employed e.g. in [1–6]. Some of them have been built around measuring the grid impedance [1–3] while others rely on the transients generated by the fault [4, 5]. Even though the problem of fault location has existed as long as power grids have, new approaches such as [6] are still being developed.

Like in many other engineering problems, cost optimization is one driving factor in grid fault location. For long, large-capacity, high-voltage transmission lines, faults have a large impact and can take long to search. It can be beneficial to install dedicated fault locator hardware on both ends of one line segment to indicate the placement of the fault [7]. For smaller lines, the incentives for installing fault location hardware decreases and it is not reasonable to have measurement hardware for each line segment. The fault location methods for distribution networks have generally been based on impedance measurement, and the methods have been developed under the assumption that measurements are only available at the substations [8–13]. These methods rely on iterations and constructing equivalent impedance models of the grid for each node. In addition to the traditional mathematical formulation, artificial intelligence (AI) has been considered for network protection [14–24]. While the approach of using AI is new, most research has been limited to the same measurement information gathered at the substation that is available for conventional methods.

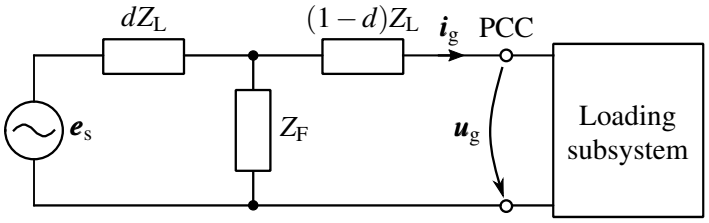

Fig. 1: Simplified model of a grid with a fault.

An additional challenge for the previously proposed impedance-based fault location methods is caused by the increasing amount of distributed generation (DG) and development towards smart grids [25]. This is because the grid impedance is calculated from voltages and currents measured at the substation. Thus, the current provided by the distributed generation might remain unknown since it does not neceessarily flow through the substation. However, distributed generation is generally connected to the grid through power electronic converters. They provide a possibility to develop new fault location methods utilizing the data gathered from several points around the grid, as the converters are active devices that have built-in sensors together with processing and communication capabilities. By using e.g. grid impedances as seen by the converters at their terminals, it might be possible to locate faults in the network without having to resort to arduous model construction and iteration. Multiple observation points offer an opportunity for pinpointing the correct fault placement from the multiple possible locations that come up when estimating fault distance from a single point.

The fault in the grid does not affect only to the grid impedance but also to the voltage: the fault causes a change in the voltage level, typically a sag. The depth of the sag relates to the distance of the fault from the observation point [26]. Thus, in addition to the impedance-based fault location, utilization of other measurements available in the converters, such as converter terminal voltage, is an interesting possibility. Utilizing data from multiple sources in analytical calculations would require even more equivalent model constructions and iteration than the proposed methods, e.g. [9]. However, AI, especially machine learning (ML), is well suited for handling large amounts of data that can be gathered from several distributed measurement points.

This paper proposes an approach of using measurements gathered from distributed converters around the grid for the purpose of locating faults. The measurement data consists of grid impedances estimated by the converters and voltages measured at their connection points, named here as the point of common coupling (PCC). Initially, faults in different test grids containing converters are simulated and analysed. The changes in the impedance estimates and measured PCC voltages are studied in relation to the location of a fault in the circuit. Finally, the simulated data is used to train a classifier based on multinomial logistic regression, a ML algorithm, to predict the placement of the fault. The accuracy of the obtained classifier is evaluated on a test data set previously unseen by the classifier.

2. Simplified Model of a Grid

In this paper, boldface letters refer to space vectors that are used for voltages and currents. A simplified one-line representation of a three-phase grid without neutral conductor is shown in Fig. 1. The grid is modelled as a voltage source $\boldsymbol{e}_s$ that supplies a loading subsystem including loads and grid-connected converters through a line impedance $Z_L(j\omega)$. In this paper, the line impedance is modelled as a series connection of a resistance R_L and an inductance L_L, i.e. $Z_L(j\omega) = R_L + j\omega L_L$. From now on, the frequency dependence of impedances is not marked. The grid voltage at the PCC, cf. Fig. 1, is referred as $\boldsymbol{u}_g$. A fault impedance Z_F splits the line impedance in two parts, dZ_L and $(1-d)Z_L$, where d is the split ratio ($0 < d < 1$, $d \in \mathbb{R}$). As a result, the grid impedance Z_g as seen from the PCC is

$$Z_g = (1-d)\,Z_L + \frac{dZ_L Z_F}{dZ_L + Z_F}. \tag{1}$$

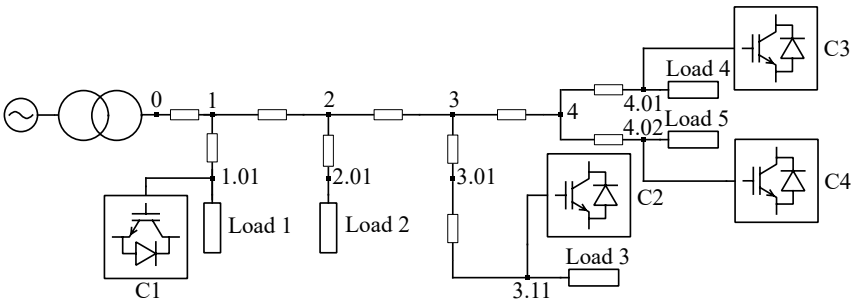

Fig. 2: Part of a grid with distributed converters.

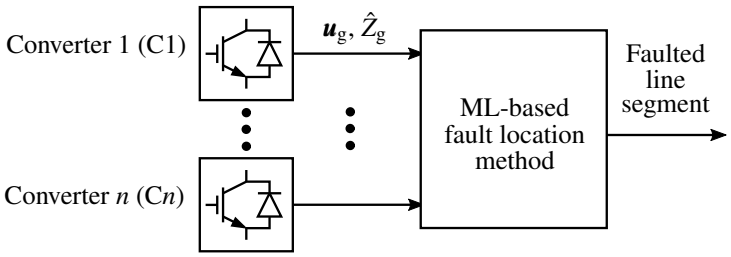

Fig. 3: Proposed fault location approach.

During normal operation, the fault impedance is infinite ($Z_F = \infty$), and the grid impedance Z_g equals to Z_L. Conversely, in the case of a finite fault impedance Z_F, the grid impedance Z_g depends on the distance of the fault from the subsystem terminals as well as on the fault impedance itself, as shown in (1). From Fig. 1 and (1), it can also be deduced that the voltage $\boldsymbol{u}_g$ and the current $\boldsymbol{i}_g$ are also affected in relation to the distance of the fault.

3. Fault Location Approach

The proposed fault location approach assumes that multiple three-phase converters are distributed in the grid. An example is shown in Fig 2. The converters can measure the grid voltage $\boldsymbol{u}_g$ and current $\boldsymbol{i}_g$, and estimate the impedance Z_g from the point they are connected to the grid. Converters used for distributed generation can be equipped with a data connection e.g. to a cloud service which can be used as a platform for the fault location algorithm. This is illustrated in Fig. 3 where the measurements and estimates from converters are fed to a ML-based fault location method.

During a fault, each converter observes a change in the grid impedance Z_g and in the magnitude of the PCC voltage $\boldsymbol{u}_g$ depending on the location of the fault relative to the converter. However, since the distribution network contains many parallel connected branches where the fault may be placed, the resulting change in the voltage or impedance estimate observed by a single converter might not be unique. That is, a similar change in the impedance or voltage may be caused by a fault in several different locations. Nevertheless, during a fault, each converter experiences different changes in the measured quantities, and these changes depend on the converter location. If the measured data from all of the converters is combined, as shown in Fig. 3, faults in different locations can lead to unique patterns that work as a basis of the proposed ML-based fault locating method.

3.1. Impedance Estimation

In this paper, the grid-impedance estimators of the converters are based on sliding discrete Fourier transform and they are implemented as in [27]. A block diagram of the converter control system with the impedance estimation method is presented in Fig. 4. The estimator injects a small amplitude excitation signal $\boldsymbol{v}_e$ to the converter voltage reference $\boldsymbol{u}_{c,ref}$ at an intermediate frequency that is not present in the power system naturally, and measures the resulting current $\boldsymbol{i}_g$ and voltage $\boldsymbol{u}_g$ at the converter connection point. The impedance estimator provides the inductance estimate $\hat{L}_g$ and the resistance estimate $\hat{R}_g$ at the injection frequency. Since the amplitude of the injected signal is very low compared to that of the

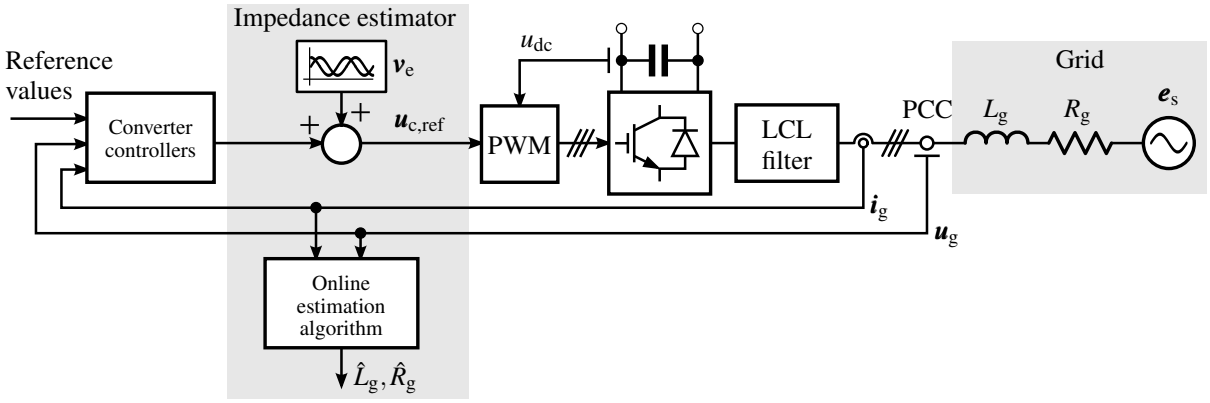

Fig. 4: Converter control system with impedance estimation [27].

grid voltage and the injection frequency is chosen to be outside of the grid harmonics, the effect of the injection signal on other components in the grid can be considered negligible. More detailed description of the estimation method can be found in [27].

3.2. Machine Learning

AI, and ML in particular, provide powerful tools for extracting insights and predictions from large amounts of data where conventional algorithms are too complex for practical use. While there is a plethora of different ML methods suitable for the task of fault prediction, the main goal of this paper is to provide a feasibility study for the proposed approach, and therefore, the multinomial logistic regression is employed due to its simplicity and relatively good performance.

In multinomial logistic regression, the output from the learning algorithm is typically called a classifier and it is a function $\hat{f} : \mathcal{X} \to \mathcal{Y}$, where $\mathcal{X}$ is the set of possible feature vectors and $\mathcal{Y}$ is the set of possible labelings. In the case of observed data, a subscript i, $i \in \{1,2,\ldots,N\}$, is added to the feature vectors and labels to distinguish the observations in a sample of size N, e.g., $\mathbf{x}_1$ and y_1 are the feature vector and the label for the first observation in a sample. In this paper, the feasibilities of three different feature vectors are explored. The first feature vector consists of proportional changes in the PCC voltages measured by each converter in the grid. The second and third feature vectors, on the other hand, consist of, respectively, the proportional changes in the inductance and resistance estimates for each converter in the grid. The reference voltages, inductances and resistances are those observed under fault-free operation. Consequently, $\mathbf{x}_i \in \mathcal{X} \subset \mathbb{R}^K$ in a grid with K converters. For an electric grid with M different line segments, the codomain $\mathcal{Y}$ is given as $\mathcal{Y} = \{1,2,\ldots,M\}$, i.e., each line segment is defined by an unique integer.

The multinomial logistic regression algorithm is based on learning M different weight vectors $\mathbf{w}_m \in \mathbb{R}^K$, $m \in \{1,2,\ldots,M\}$, which are then used to compute the probability of the observation $\mathbf{x}_i$ having the label m, i.e., $p(m\,|\,\mathbf{x}_i)$. This probability is computed as [28]

$$p(m\,|\,\mathbf{x}_i) = \frac{\exp\left(\mathbf{w}_m^{\mathrm{T}}\mathbf{x}_i\right)}{\sum_{k=1}^{M}\exp\left(\mathbf{w}_k^{\mathrm{T}}\mathbf{x}_i\right)} \tag{2}$$

where the superscript T denotes the transpose operator. The classifier $\hat{f}$ can then be written using the above probabilities as

$$\hat{f}(\mathbf{x}_i) = \arg\max_m p(m\,|\,\mathbf{x}_i). \tag{3}$$

In essence, the use of the multinomial logistic regression algorithm consists of the following steps:

1. A set of N simulations is carried out under different fault conditions.

2. From each simulation, indexed as $i \in \{1,2,\ldots,N\}$, a feature vector $\mathbf{x}_i$ is collected, which consists of either proportional differences in the PCC voltages measured, or in the grid inductances or resistances estimated by each converter.

3. For an electric grid with M line segments, each simulation case is given an integer label y_i between 1 and M, which maps to a unique line segment.

4. The set of N tuples $(\mathbf{x}_i, y_i)$ is used to train the classifier $\hat{f}$ by minimizing the cross-entropy error function, defined as [28]

$$\mathcal{E}(\mathbf{w}_1, \mathbf{w}_2, \ldots, \mathbf{w}_M) = -\sum_{n=1}^{N}\sum_{m=1}^{M} t_{nm} \log[p(m\,|\,\mathbf{x}_n)] \tag{4}$$

   where $t_{nm} = 1$ if the nth observation has label m, i.e., $y_n = m$, and otherwise $t_{nm} = 0$.

5. The obtained classifier $\hat{f}$ is used to predict the fault location on previously unseen data.

4. Simulation study

The proposed fault location approach is studied through simulations by using Simulink with PLECS blockset. A low-voltage (400 V, 50 Hz) distribution grid of a residental area, shown in Fig. 5, is considered. In the figure, the numbers refer to nodes acting either as connection points between two or more line segments or as consumption points, e.g., buildings. The grid is fed through a 315 kVA transformer that is located in node 0. Symbols C1 - C7 refer to converters representing distributed generation, e.g. rooftop photovoltaics. Their nominal powers are, respectively, 5 kVA, 4 kVA, 4 kVA, 8 kVA, 5 kVA, 5 kVA, and 4 kVA. The converters are connected to the nodes with underlined numbers. Furthermore, the colours indicate the unit impedance of each line segment. In the simulations, each converter estimates the grid inductance and resistance as seen from its terminals and measures the magnitude of the PCC voltage at the connection point for the three different feature vectors $\mathbf{x}_i$ under study. These vectors are then used to train the ML classifier (3) with the multinomial logistic regression algorithm. The trained classifier can then be used to predict the fault location based on the input feature vector. The fault location algorithm is implemented using the scikit-learn package in Python [29]. For the impedance estimation, each of the converters use an 8 V injection signal. In order to prevent disturbances caused by the injection signals from other converters connected to the same grid, the frequency of the injection voltage is unique for each of the converters. The injection frequencies 110 Hz, 120 Hz, 130 Hz, 140 Hz, 160 Hz, 170 Hz, and 180 Hz, are used by the converters C1 - C7, respectively.

4.1. Simplified Test Grid

First, a simplified version of the upper branch of Fig. 5, shown in Fig. 2, is studied through simulations. Initially, the non-faulted grid simulations are carried out to determine the reference voltages and inductances. They are followed by the simulations studying the effect of three-phase short-circuit as seen by the converters. A prerequisite for the ML-based fault location method is to have sufficiently distinct data patterns under different faults. Therefore, the changes in grid voltage magnitudes and impedance estimates gathered from the converters are examined under various fault conditions.

Each simulation round has a unique location for the fault. That is, all the line segments are divided evenly into 10 parts, and a fault in each location is simulated separately. The simulated fault impedance is purely resistive with a value of $R_\mathrm{F} = 0.2$ p.u.

Fig. 6(a) - (c) shows the simulation results presenting the observed changes in the inductance and resistance estimates, and PCC voltage magnitudes. The y axis in the figures presents the percentual change in the estimated or measured quantity during the fault condition in comparison with the non-faulted situation.

Figures 6(a) and 6(b) show that the inductance estimates change more consistently than the resistance estimates. That is, in all of the simulated cases, the estimated inductances are lower in the fault situation

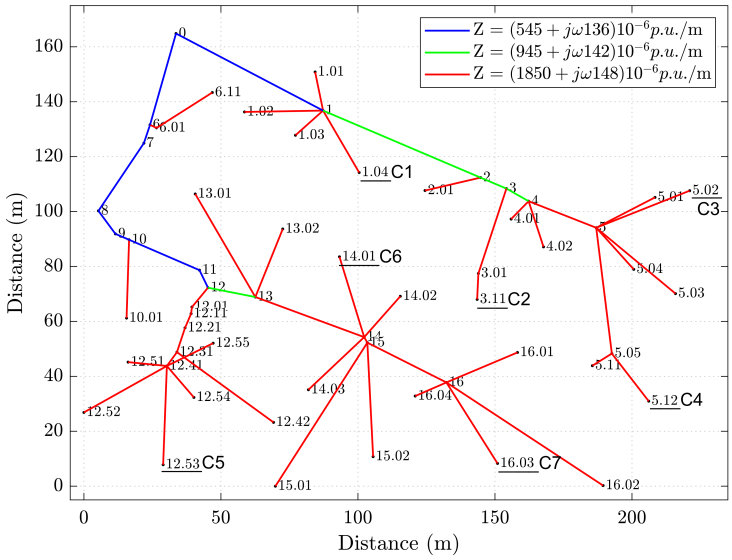

Fig. 5: Distribution grid.

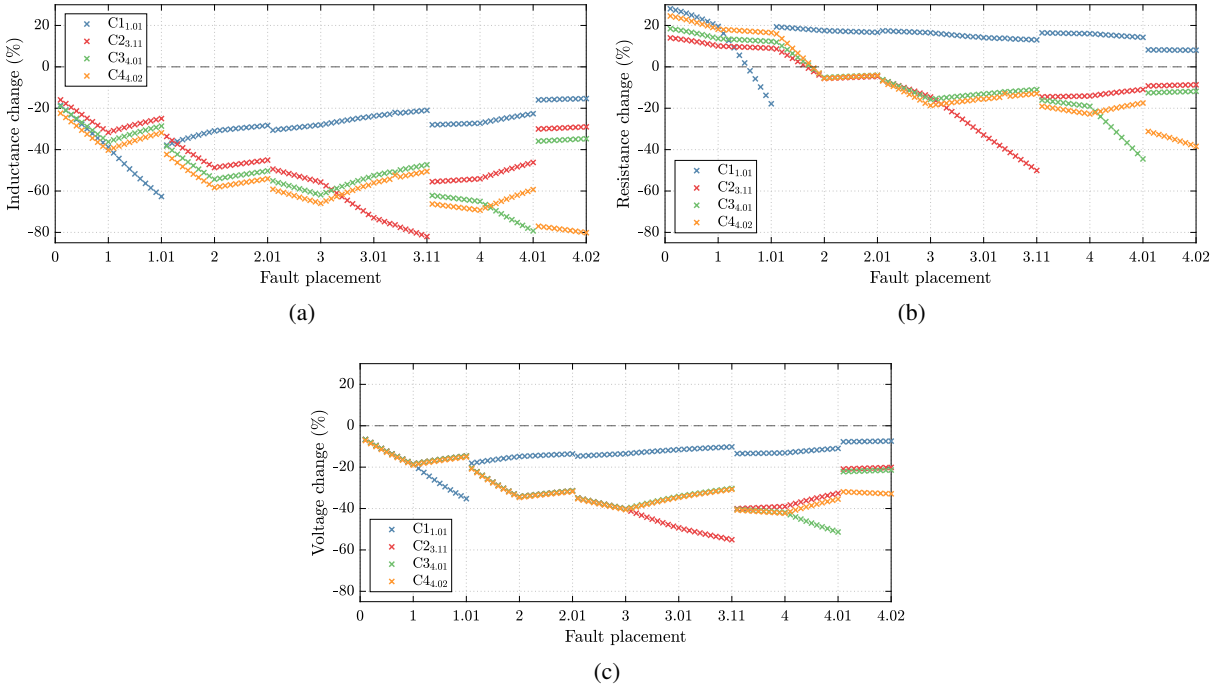

Fig. 6: Percentual change observed by the converters in the (a) inductance estimate $\hat{L}_{\mathrm{g}}$, (b) resistance estimate $\hat{R}_{\mathrm{g}}$, and (c) PCC voltage magnitude $|\boldsymbol{u}_{\mathrm{g}}|$. Horizontal-axis labels refer to node numbers in Fig. 2. Between the node numbers (line segment), the axis is uniformly distributed between 0 and 1 corresponding to the fault location d in the line segment.

than during normal operation. On the contrary, the resistance estimates are in many cases higher during faults than in normal operation. This is expected, since in the simulated cases the fault is purely resistive element, meaning that the resistance estimates from the converters contain also the fault resistance.

Changes in the measured PCC voltages are presented in Fig. 6(c). While the magnitude of the observed changes in the inductance estimates and the PCC voltages differ, the curve shapes in Fig. 6(a) and Fig. 6(c) are similar.

Results indicate that when the fault is upstream from the converter, i.e. the fault lies between the supply and the converter, the shorter distance is seen as a larger change in both the impedance estimated and

PCC voltage measured by the converter. This is expected based on Eq. (1). Conversely, from a single converter point of view, the changes in the estimates and measurements are nearly indistinguishable from each other regardless of the fault location when the fault lies downstream from the converter. Based on Fig. 6(a) and Fig. 6(c), the changes in the inductances might be better features to be used in the ML algorithm than the changes in the PCC voltages, since the first seems to result in more distinguishable feature pattern. Furthermore, since the faults are typically resistive, the use of inductance estimates should be preffered over the resistance estimates in developing the fault location algorithm [30].

4.2. Fault Location in Distribution Grid

The simulations with the simplified test grid resulted in unique feature patterns. In this subsection, the more complicated distribution grid shown in Fig. 5 is simulated and the ML-based fault location algorithm is trained and tested.

The simulated network has a counterpart in reality, but without any converters. Thus, the grid parameters in the simulation model were selected accordingly. The grid shown in Fig. 5 has two main branches and several line taps with a total of 33 loads and $M = 57$ line segments. Balanced, three-phase loads are assumed. The loading conditions in the simulations represent typical power consumption of each of the load nodes in the real grid. The powers of the loads are between 3 kVA and 10 kVA (0.01 ... 0.03 p.u.). The $K = 7$ converters are spread randomly to the consumption nodes, i.e., the endpoint nodes, in the grid. The converter ratings were selected based on the load at the node rounded down to the closest kVA. In the simulations, each of the converters operate with the nominal power.

First, a training data set for the ML-based fault location algorithm was generated. A symmetric resistive three-phase fault ($R_\mathrm{F} = 0.2$ p.u.) was simulated in every line segment at different locations. For over 10 m long line segments, the fault location $d = [0.2, 0.5, 0.8]$ and for shorter line segments, $d = 0.5$ was used. The total number of simulations was $N = 147$. The training data, containing the relative changes observed by each converter are presented in Fig. 7 (a) - (c), for inductance estimate, resistance estimate, and PCC voltage, respectively.

Second, a validation data set for the fault location algorithm was generated. The validation data was generated by simulating a fault in different locations and collecting the data from the converters. Both symmetric ($R_\mathrm{F} = [0.002, 0.2, 2.0, 20]$ p.u.) and asymmetric ($R_\mathrm{F} = 0.2$ p.u. between phases a and b) resistive faults were simulated. Each of the defined faults was simulated separately in three random locations in each of the line segments over 10 m long, and in a single random location in each of the shorter line segments. The loading condition in the grid was also varied between the simulations.

Fig. 8 (a) - (b) presents the prediction accuracy of fault location for the various fault conditions included in the validation data set described above. Fig. 8(a) shows the prediction accuracy when the ML algorithm indicates the faulting line segment correctly, while in Fig. 8(b) predictions to the line segments next to the actual one are also considered as correct predictions.

The results show that when the fault resistance is the same as in the training data set but the fault location and grid loading condition are randomized, the accuracy of the predictions is good. Considering that the test grid has several short branches and only a few converters, the capability to correctly identify the area where the fault happens is a desirable result. When the fault resistance differs from the training data, the amount of correct fault location predictions drops drastically, especially when the resistance estimate is used. The last one is reasonable, since the resistance estimate is affected by the fault resistance. However, using either of the three feature vectors, it is still possible to find the general area where the fault is located quite reliably. The asymmetric phase-to-phase fault shows interesting results. Using inductance change, it is possible to pinpoint the correct fault placement in significant majority of the cases. Since the voltages are averaged across all three phases in this approach, the PCC voltage measurement is less accurate for unbalanced faults.

The results obtained using the voltage measurement are generally very close to the ones obtained using the inductance estimate, despite the overlap of observed changes seen in Figs. 6 and 7. This is possible due to the topology of the network under observation. Not all converters provide significant information in all fault situations, so even overlapping results are enough to differentiate between fault placements.

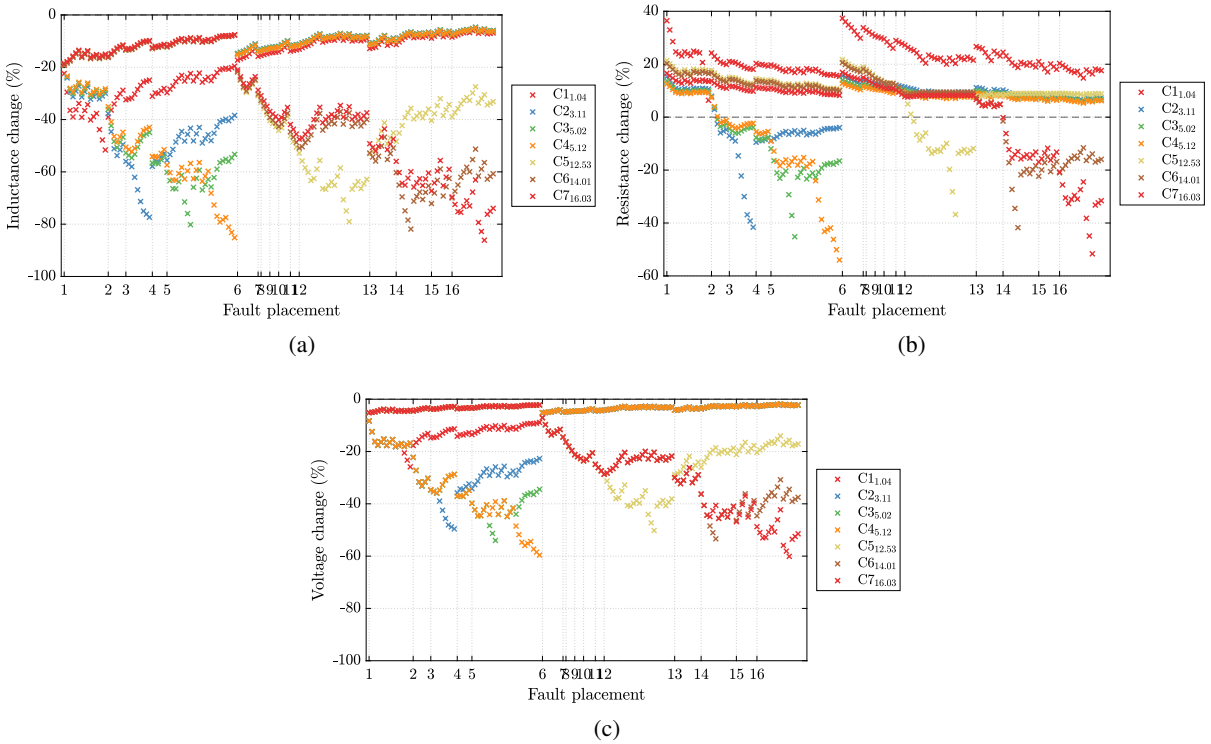

Fig. 7: Percentual change observed by the converters in (a) inductance estimate $\hat{L}_{\mathrm{g}}$, (b) resistance estimate $\hat{R}_{\mathrm{g}}$, and (c) PCC voltage magnitude $|\boldsymbol{u}_{\mathrm{g}}|$. Horizontal-axis labels refer to the node numbers in Fig. 5. Between the node numbers (line segment), the axis is uniformly distributed between 0 and 1 corresponding to the fault location d in the line segment.

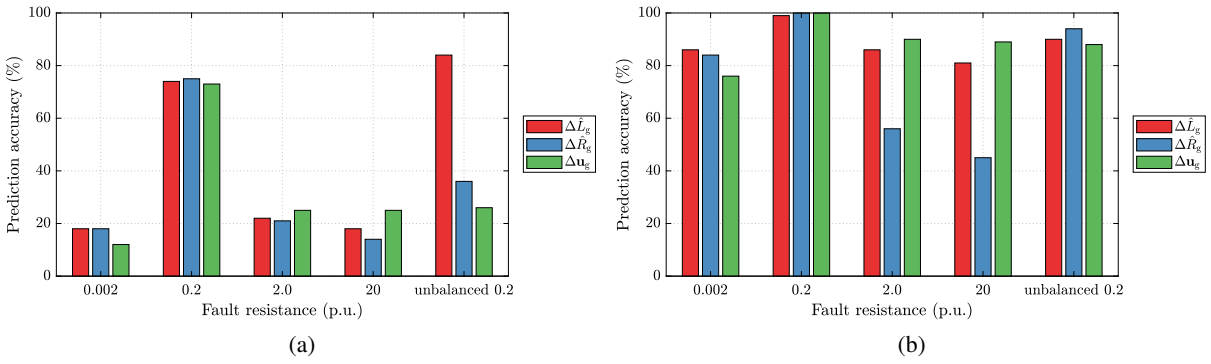

Fig. 8: Accuracy of the fault location with different fault resistances, when (a) only the correct predictions are accepted, and (b) when the predictions in the line segments next to the correct one are accepted.

5. Conclusions

This paper proposed an approach for locating faults in a distribution grid utilizing data gathered from distributed converters. The approach was based on a ML algorithm that utilized either the grid inductance or resistance estimates, or the PCC voltage measurements. The results indicated good accuracy in the prediction of the fault location in the selected distribution grid.

According to the results, inductance estimates produce more distinguishable patterns and consistent results than PCC voltage measurements. However, they provide quite similar prediction accuracy for the fault location. It was noticed that resistance estimates are affected by the fault resistance, and thus the prediction accuracy decreases when the actual fault resistance differs from the training data. An important finding was also that the ML algorithm was able to locate asymmetric faults based on the inductance estimates. However, the fault location based on the PCC voltage measurement might be more preferable

choice, since it does not require any signal injection which needs to have unique frequencies for each of the converters, and moreover, which may cause disturbances in the grid.

In this paper, the main goal was to provide a feasibility study for the proposed approach. Therefore, the multinomial logistic regression that is known to be simple and offer relatively good performance, was used. In the future studies, in order to improve the prediction accuracy, other ML approaches, such as the support vector machine (SVM), could be applied. The prediction accuracy could also be improved e.g. by pre-processing the input features, such as filtering only the relevant features for each label. In the future, utilization of more complicated feature vectors, including e.g. both the PCC voltages and the grid currents, should be studied.

References

[1] T. Takagi, Y. Yamakoshi, J. Baba, K. Uemura, and T. Sakaguchi, "A new algorithm of an accurate fault location for EHV/UHV transmission lines: Part I–Fourier transformation method," *IEEE Transactions on Power Apparatus and Systems*, vol. PAS-100, no. 3, pp. 1316–1323, 1981.

[2] L. Eriksson, M. M. Saha, and G. Rockefeller, "An accurate fault locator with compensation for apparent reactance in the fault resistance resulting from remore-end infeed," *IEEE Transactions on Power Apparatus and Systems*, vol. PAS-104, no. 2, pp. 423–436, 1985.

[3] D. A. Tziouvaras, J. B. Roberts, and G. Benmouyal, "New multi-ended fault location design for two-or three-terminal lines," in *Proc. International Conference on Developments in Power System Protection (IEE)*, Amsterdam, Netherlands, Apr. 2001, pp. 395–398.

[4] M. Korkali, H. Lev-Ari, and A. Abur, "Traveling-wave-based fault-location technique for transmission grids via wide-area synchronized voltage measurements," *IEEE Transactions on Power Systems*, vol. 27, no. 2, pp. 1003–1011, 2011.

[5] M. Nazari-Heris and B. Mohammadi-Ivatloo, "Application of heuristic algorithms to optimal PMU placement in electric power systems: an updated review," *Renewable and Sustainable Energy Reviews*, vol. 50, pp. 214–228, 2015.

[6] D. Topolanek, M. Lehtonen, P. Toman, J. Orsagova, and J. Drapela, "An earth fault location method based on negative sequence voltage changes at low voltage side of distribution transformers," *International Journal of Electrical Power & Energy Systems*, vol. 118, pp. 1–8, 2020.

[7] M. M. Saha, J. J. Izykowski, and E. Rosolowski, *Fault location on power networks*. Springer Science & Business Media, 2009.

[8] J. Mora-Florez, J. Melendez, and G. Carrillo-Caicedo, "Comparison of impedance based fault location methods for power distribution systems," *Electric Power Systems Research*, vol. 78, no. 4, pp. 657–666, 2008.

[9] R. Dāsa, "Determining the locations of faults in distribution systems," Ph.D. dissertation, University of Saskatchewan, 1998.

[10] S.-J. Lee, M.-S. Choi, S.-H. Kang, B.-G. Jin, D.-S. Lee, B.-S. Ahn, N.-S. Yoon, H.-Y. Kim, and S.-B. Wee, "An intelligent and efficient fault location and diagnosis scheme for radial distribution systems," *IEEE Transactions on Power Delivery*, vol. 19, no. 2, pp. 524–532, 2004.

[11] R. H. Salim, M. Resener, A. D. Filomena, K. R. C. De Oliveira, and A. S. Bretas, "Extended fault-location formulation for power distribution systems," *IEEE Transactions on Power Delivery*, vol. 24, no. 2, pp. 508–516, 2009.

[12] H. K. Jahanger, M. Sumner, and D. W. Thomas, "Influence of DGs on the single-ended impedance based fault location technique," in *Proc. IEEE International Conference on Electrical Systems for Aircraft, Railway, Ship Propulsion and Road Vehicles & International Transportation Electrification Conference (ESARS-ITEC)*, Nottingham, UK, Jan. 2018, pp. 1–5.

[13] F. Aboshady, D. Thomas, and M. Sumner, "A new single end wideband impedance based fault location scheme for distribution systems," *Electric Power Systems Research*, vol. 173, pp. 263–270, 2019.

[14] S. Gururajapathy, H. Mokhlis, and H. Illias, "Fault location and detection techniques in power distribution systems with distributed generation: A review," *Renewable and Sustainable Energy Reviews*, vol. 74, pp. 949 – 958, 2017.

[15] M. Kezunovic, "A survey of neural net applications to protective relaying and fault analysis," *Engineering Intelligent Systems for Electrical Engineering and Communications*, vol. 5, pp. 185–192, 1997.

[16] S. A. M. Javadian, A. M. Nasrabadi, M. . Haghifam, and J. Rezvantalab, "Determining fault's type and accurate location in distribution systems with DG using MLP neural networks," in *Proc. International Conference on Clean Electrical Power*, Capri, Italy, Jun. 2009, pp. 284–289.

[17] R. Salat and S. Osowski, "Accurate fault location in the power transmission line using support vector machine approach," *IEEE Transactions on Power Systems*, vol. 19, no. 2, pp. 979–986, 2004.

[18] B. Ravikumar, D. Thukaram, and H. Khincha, "Knowledge-based approach using support vector machine for transmission line distance relay co-ordination," *Journal of Electrical Engineering and Technology*, vol. 3, no. 3, pp. 363–372, 2008.

[19] B. Das, "Fuzzy logic-based fault-type identification in unbalanced radial power distribution system," *IEEE Transactions on Power Delivery*, vol. 21, no. 1, pp. 278–285, 2005.

[20] S. Adhikari, N. Sinha, and T. Dorendrajit, "Fuzzy logic based on-line fault detection and classification in transmission line," *SpringerPlus*, vol. 5, pp. 1–14, 2016.

[21] P. P. Bedekar, S. R. Bhide, and V. S. Kale, "Fault section estimation in power system using Hebb's rule and continuous genetic algorithm," *International Journal of Electrical Power & Energy Systems*, vol. 33, no. 3, pp. 457–465, 2011.

[22] Q. Jin and R. Ju, "Fault location for distribution network based on genetic algorithm and stage treatment," in *Proc. Spring Congress on Engineering and Technology*, Xi'an, China, May 2012, pp. 1–4.

[23] H. Mokhlis and H. Li, "Non-linear representation of voltage sag profiles for fault location in distribution networks," *International Journal of Electrical Power & Energy Systems*, vol. 33, no. 1, pp. 124–130, 2011.

[24] L. J. Awalin, H. Mokhlis, and A. Halim, "Improved fault location on distribution network based on multiple measurements of voltage sags pattern," in *Proc. IEEE International Conference on Power and Energy (PECon)*, Kota Kinabalu, Malaysia, Dec. 2012, pp. 767–772.

[25] C. M. Furse, M. Kafal, R. Razzaghi, and Y.-J. Shin, "Fault diagnosis for electrical systems and power networks: A review," *IEEE Sensors Journal*, vol. 21, no. 2, pp. 888–906, 2021.

[26] P. Heine and M. Lehtonen, "Voltage sag distributions caused by power system faults," *IEEE Transactions on Power Systems*, vol. 18, no. 4, pp. 1367–1373, 2003.

[27] J. Kukkola, M. Routimo, and M. Hinkkanen, "Real-time grid impedance estimation using a converter," in *Proc. IEEE Energy Conversion Congress and Exposition (ECCE)*, Baltimore, MD, USA, Sep./Oct. 2019, pp. 6005–6012.

[28] C. M. Bishop, *Pattern Recognition and Machine Learning*. Springer, 2006.

[29] F. Pedregosa, G. Varoquaux, A. Gramfort, V. Michel, B. Thirion, O. Grisel, M. Blondel, P. Prettenhofer, R. Weiss, V. Dubourg, J. Vanderplas, A. Passos, D. Cournapeau, M. Brucher, M. Perrot, and E. Duchesnay, "Scikit-learn: Machine learning in Python," *Journal of Machine Learning Research*, vol. 12, pp. 2825–2830, 2011.

[30] S. Hänninen, "Single phase earth faults in high impedance grounded networks : characteristics, indication and location," Doctoral thesis, 2001.